2008 10th Intl. Conf. on Control, Automation, Robotics and Vision
Hanoi, Vietnam, 17–20 December 2008

A Vision-based Approach for Surface Roughness Assessment at Micro and Nano scales

Ghassan A. Al-Kindi
Department of Mechanical Engineering
University of Technology
Baghdad, Iraq

Bijan Shirinzadeh, Yongmin Zhong
Robotics & Mechatronics Research Laboratory
Department of Mechanical and Aerospace Engineering
Monash University

***Abstract*—This paper presents a vision-based approach for valid assessment of surface roughness in both micro-scale and nano-scale regions. To enable data comparisons, three sets of surface data in the micro and nano regions are acquired by using a CCD camera, a video-based optical microscope and a stylus instrument. Data filtering and analysis procedures are applied to the acquired data. Results for computation of roughness parameters by using vision data provide adequate values for assessment of surface roughness in the manner as similar as stylus based technique. No obvious changes in the computed roughness parameter values are resulted from the micro and nano regions. In the nano region, a cavity graphs technique provides distinguishable forms of graphs that tend to more gradual increase of the cavity percentage to denote the collection of the macro surface details. In addition, an auto correlation technique applied in the nano region succeeds to discriminate the surface irregularities relationship with respect to their periodicity and randomness. The overall acquired results indicate that vision systems are a valid source of data for reliable surface roughness evaluation in both micro/nano-scale regions. The results are very useful in achieving commercial 3D vision based micro-nano roughness measurement systems for industrial applications.**

Keywords—**machine vision, surface roughness measurement, image acquisition and analysis, and micro and nano-scale regions**

I. INTRODUCTION

The commonly used method for surface roughness measurement in industrial applications is the direct method by using a measuring stylus [1]. Stylus techniques have great inherent limitations, such as the fragility of the instrument, the possible surface scratching, and the limited accuracy due to probe tip radius. In addition, stylus techniques are also used for acquiring 2D surface topography [2].

The development of non-contact based roughness measurement techniques for engineering surfaces has received considerable attentions. The non-contact based roughness measurement techniques aim to find alternative ways to permit rapid surface roughness measurements with accepted accuracy. One of the most promising non-contact based roughness measurement techniques is the computer vision technique [3]. However, practical surface roughness measurement based on computer vision technology is still difficult [4].

Bradly and Wong [5] developed a method to monitor surface texture of the work-piece for on-line tool condition assessment in milling operations, in which spatial and frequency domains are used. Lee et al [6] presented a method to assess surface roughness by using texture features of image data. Tasan et al [7] proposed a wear measurement technique based on the comparison of local surface heights gained from image data. Al-Kindi et al [8] combined spacing and amplitude parameters obtained from the grey level profiles to obtain an evaluation parameter. Ramana and Ramamoothy [9] presented a grey-level difference matrix for texture analysis. Kruger-Sehm and Perez [10] presented a guideline for the calibration of interference microscopes by using the same items, which were successfully applied in the guidelines for stylus instruments. Udupa et al [11] studied the performance of a scanning optical microscope for obtaining roughness measures of micro/macro surface irregularities. Kuriyagawa et al [12] investigated the formation mechanism of nano-topography on axisymmetric ground surfaces.

This paper presents a computer vision based methodology for surface roughness assessment in both micro/nano-scale regions. The obtained results may open a way to establish vision-based surface roughness measurement systems for both micro-scale and nano-scale regions.

II. ROUGHNESS MEASUREMENT

The most popular technique for roughness measurement is to use surface assessing parameters. The centre line average parameter Ra is frequently used and it is the most industrially recognized parameter. However, the parameter Ra is not capable alone to distinguish changes in surfaces [13]. Therefore, many other assessment parameters and methods were developed over the years to enable improved ways of surface roughness evaluation.

The common technique in computation of the surface assessing parameters is based on the computation of signal departure from mean. Acquired data arrays that represent the full evaluation length are usually divided into five sub-arrays of equal number of samples to enable better statistical analysis. These sub-arrays are referred to as the sampling length arrays.

Reference mean lines are commonly implemented in the computation of surface roughness parameters. The most common line used as a reference line is the Least Squares Mean Line in which the areas of the profile above and below this line are equal and the sum of the squares of the deviations of the profile from this line is minimized. Therefore, if F and f present the filtered data array of the full evaluation length and the sampling length, respectively, and C presents the mean line, the departure data array G and sub-arrays gi from the mean line are computed by:

$$G(n) = F(n) - C \tag{1}$$

and

$$g_i(m) = f_i(m) - C \tag{2}$$

where n=1,2,3,…,N, i=1 to 5, and m=1,2,3,…,N/5. N represents the total number of elements in the evaluation length array F.

Table 1. Adopted surface roughness parameters

Parameter Name	Parameter Definition
Centre Line Average Parameter	$R_a = \frac{1}{N}\sum_{n=1}^{N}\lvert G(n)\rvert$
Root Mean Square Parameter	$R_q = \sqrt{\frac{1}{N}\sum_{n=1}^{N} G^2(n)}$
Maximum Peak to Valley Set of Parameters	$R_{ti} = \max_{m=1,2,3,\ldots,N/5}(g_i(m)) - \min_{m=1,2,3,\ldots,N/5}(g_i(m))$ $R_t = \max_{n=1,2,3,\ldots,N}(G(n)) - \min_{n=1,2,3,\ldots,N}(G(n))$ $R_{tm} = \frac{1}{5}\sum_{i=1}^{5} R_{ti}(i)$
Maximum Valley Depth Set of Parameters	$R_{vmax}(i) = \max_{m=1,2,3,\ldots,N/5}(C - g_i(m))$ $R_v = \frac{1}{5}\sum_{i=1}^{5} R_{vmax}(i)$
Maximum Peak Height Set of Parameters	$R_{pmax}(i) = \max_{m=1,2,3,\ldots,N/5}(g_i(m) - C)$ $R_p = \frac{1}{5}\sum_{i=1}^{5} R_{pmax}(i)$
Skewness Parameter	$R_{sk} = \frac{1}{R_q^3} \times \frac{1}{N}\sum_{n=1}^{N} G^3(n)$
Kurtosis Parameter	$R_{ku} = \frac{1}{R_q^4} \times \frac{1}{N}\sum_{n=1}^{N} G^4(n)$
RMS-Slope Hybrid Parameter	$R\Delta_q = \sqrt{\frac{1}{N}\sum_{n=1}^{N}(\theta(n) - \bar{\theta})^2}$ where $\bar{\theta} = \frac{1}{N}\sum_{n=1}^{N}\theta(n)$ $\theta = \frac{G(n) - G(n+1)}{\text{Sampling Rate}}$

The different types of roughness assessment parameters used for achieving the goal of this work is illustrated in Table 1. In addition, two techniques based on the probability density and the autocorrelation functions are also used to assess the capacity in discrimination of the different types of surface irregularities in both micro-scale and nano-scale regions.

The probability density function PDF is one of the important analytical tools that can be utilised in surface topography assessment. The cavity graph can be obtained by application of the PDF. The graph characterises the metal-cavity volumetric relationship of the surface irregularities. The cavity graph (CG) can be obtained as follows:

$$CG(t_i) = \sum_{s=1}^{t_i} \frac{1}{N} \times \underset{n=1 \text{ to } N}{\text{Count}}\{F(n) \in s\} \tag{3}$$

where ti represents the interval array that has I number of elements, and I is calculated as:

$$I = \frac{\max(F(n)) - \min(F(n))}{\text{Selected Amplitude Interval}} \tag{4}$$

The ACF is particularly useful for looking at random surfaces because it indicates:

- How quickly the random signal or processes changes with respect to the time function;
- Whether the process has a periodic component.

The ACF can be obtained by the following:

$$ACF(n) = \sum_{r=0}^{R-1} F(r)F(r+n) \tag{5}$$

III. SYSTEM SETUP

As shown in Fig. 1, a Surtronic 3P stylus-based surface roughness measuring machine manufactured by Taylor Hobson (UK) is used. In order to enable further analysis of surface profiles, the Surtronic 3P instrument is successfully interfaced to a PC by using a National Instrument PCI-6013 data acquisition card.

A Pulnix TM 300 monochrome CCD camera equipped with a 25 mm 1:1.4 F Cosmicar television lens is used to enable image data acquisition in the micro-scale region. The camera is interfaced to a PC by using a Data Translation frame grabber (Type DT-3152). This frame grabber enables the interfacing of multiple cameras. The images are digitized in a resolution of (768×576) pixels with 256 available grey levels. A resolution of 12.5 micrometers per pixel is achieved by using the vision system. To enable the roughness assessment in the nano-scale region, a video optical microscope system is used as part of the employed hardware. A second Pulnix TM-300 monochrome CCD camera is interfaced to the frame grabber card. A resolution of 400 nanometre per pixel is achieved by using the experimental setup. Fig. 1 shows the employed equipment setup.

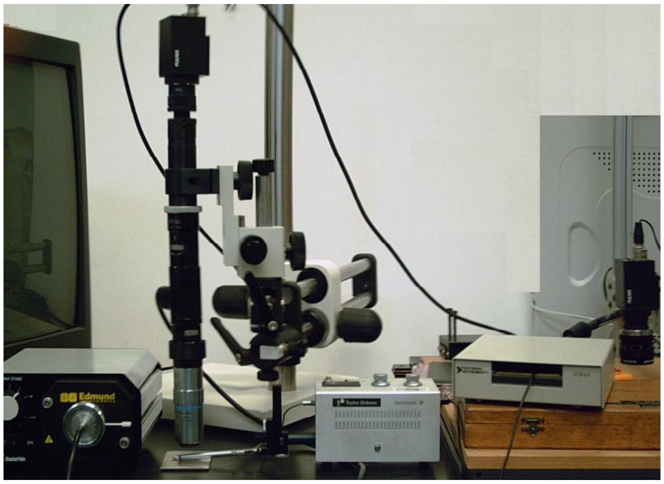

Figure 1. Equipment setup

IV. IMAGE DATA IMPLEMENTATION

In general, a continuous image scene could be approximated by equally spaced samples arranged in the form of a two dimensional array a(x,y). The term image is therefore refers to a 2D light-intensity function, denoted by a(x, y), where the value for the amplitude of (a) at spatial coordinates (x, y) gives the intensity (brightness) of the image at that coordinate:

$$a(x, y) = z \tag{6}$$

where z is the light irradiance intensity and is within the range ($0 \leq z \leq Z\text{-}1$). The interval {0, Z-1} is called the grey scale that includes a set of numbers of discrete grey levels.

The basic nature of the image data could be characterized by the incident light on the object and the surface profile. To eliminate the influence of variation in lighting, ambient light is used in the experimental work of the micro-scale vision data. It is assumed here that ambient light presents a uniform lighting that intercepts the object surface from all valid angles; surface irradiance is therefore assumed to be a characteristic of the surface topography:

$$F(n) \propto a(n) \tag{7}$$

where F(n) represents the surface height of topography data array and a(n) represents the corresponding vision-based line scan image data array.

For the nano-scale vision data, since the use of optical lighting is essential to acquire the surface data, a dedicated smoothing technique based on a moving window filter is applied to the nano-scale data in order to reduce the lighting variation:

$$\bar{a}(x, y) = a(x, y) - \frac{1}{K} \times \frac{1}{L} \sum_{l=y-\frac{L}{2}}^{y+\frac{L}{2}-1} \sum_{k=x-\frac{K}{2}}^{x+\frac{K}{2}-1} a(l, k) \tag{8}$$

where L and K are the window sizes of the filter, and they are selected to have an identical value of 80 pixels.

The adopted model to interpret the vision data implies that the normalized values of pixel intensities within the image have a linear compatibility relationship with the normalized values of the surface height topography. The discrete values of the grey scale z are therefore assumed to be equally spaced between 0 and 1 to comply with the surface height topography of the object.

In order to enable valid roughness measurements, the grey scale z of the image data is therefore normalized to cover the resulting range of the surface profile:

$$F(n) = \lambda a_{Norm}(n) \tag{9}$$

where λ represents the ratio of the obtained R_a value of the vision data to the real R_a value of the specimen profile.

V. EXPERIMENTAL RESULTS AND DISCUSSION

In this work, four sets of excellent surface finish specimens are used in the investigation. Each set includes two specimens of different roughness. These specimens are prepared by using four types of common techniques of machining, namely turning, reaming, grinding, and lapping; hence, each set of specimens has its distinct surface appearance. Fig. 2 and Fig. 3 illustrate the resulting 3D representation of the surface topography acquired from captured images, where the micro-scale views are 1.25 x 1.25 mm^2 and the nano-scale views are 40 x 40 µm. It is obvious from these figures that the micro-region images possess less height information with respect to the surface irregularities because the employed specimens have highly finished surfaces. However, in the case of the nano-scale regions, the acquired 3D surface representations ensure that the image data inherit vital information of the surface topography.

The specimens are preliminarily assessed by using the built-in module of the stylus instrument employed. Table 2 lists the obtained average R_a values together with the percentage ratio of the Standard Deviation to the mean value of the measured R_a values. Results of acquired R_a values demonstrate the high quality of the specimen's surface finish.

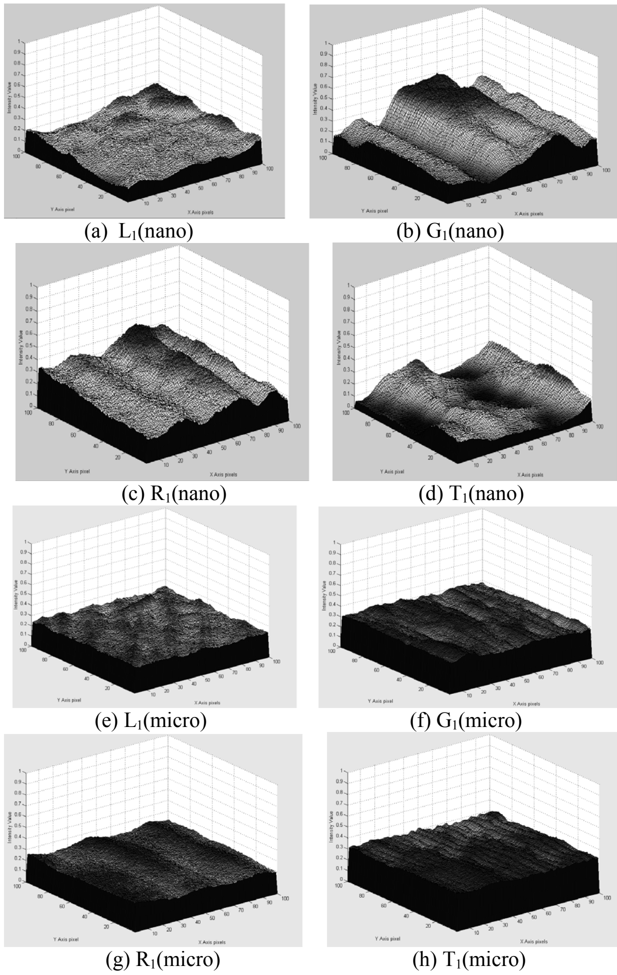

(a) L_1(nano) (b) G_1(nano)
(c) R_1(nano) (d) T_1(nano)
(e) L_1(micro) (f) G_1(micro)
(g) R_1(micro) (h) T_1(micro)

Figure 2. Acquired 3D representations of the first specimen's surfaces

Table 2. The specimens used in the experimental work

Specimen code	Machining type used	Average R_a (μm)	R_a (SD/Mean)%
T_1	Turning	1.942	1.92
T_2	Turning	0.908	5.82
G_1	Surface Grinding	0.815	12.24
G_2	Surface Grinding	0.435	16.91
R_1	Reaming	1.266	9.19
R_2	Reaming	0.523	5.61
L_1	Lapping	0.138	23.8
L_2	Lapping	0.078	11.49

Three different sets of surface data namely stylus-based, vision-based within the micro-scale, and vision-based in the nano-scale data are used in the experimental work. The three sets of data are obtained from each of the eight specimens used in the investigation.

Computational results of the adopted surface roughness parameters are given in Fig. 4. These results indicate that the provided values of the R_q, R_{tm}, R_v, R_p, R_{ku}, and the $R_{\Delta q}$ for both micro-scale and nano-scale vision data are very close to the corresponding values obtained by the stylus technique. This guarantees the validity of the proposed technique for acquiring the stated parameters. These parameters also indicate that there is no obvious change in the obtained parameters values for micro/nano-scale surface topography of the examined specimens. For the R_t parameter, a noticeable difference in the obtained values can be observed. This is because the R_t parameter can be affected by local maximum peak or local maximum valley. Thus, this makes this parameter very sensitive to singular change in the surface profile data. It is also worthy to be noted that in some of the trials, the R_{sk} parameter provides values with different signs in comparison to the stylus-based values. This indicates that vision data cannot guarantee to provide comparable values of this parameter with stylus based values, since the definition of this parameter involves a third-order model and it represents sensitivity to minor changes in the magnitude of local elements.

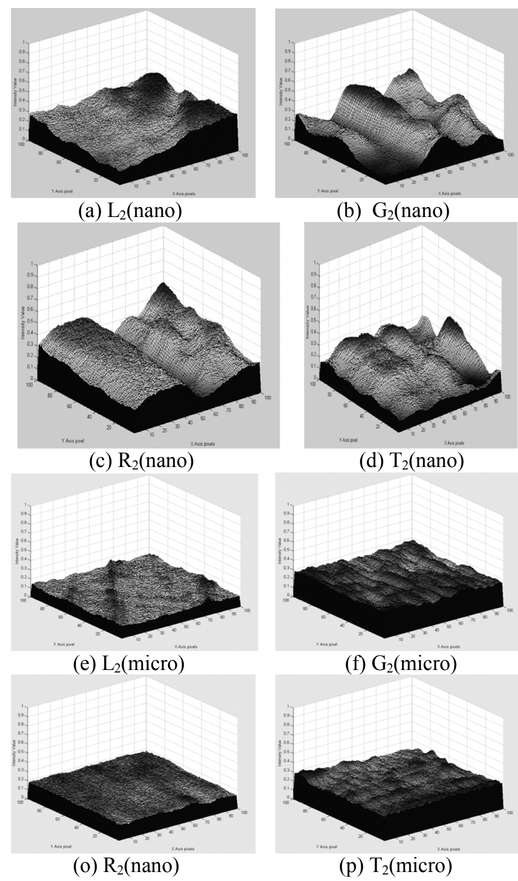

(a) L_2(nano) (b) G_2(nano)
(c) R_2(nano) (d) T_2(nano)
(e) L_2(micro) (f) G_2(micro)
(o) R_2(nano) (p) T_2(micro)

Figure 3. Acquired 3D representations of the second specimen's surfaces

Results on computation of the roughness parameters also indicates that the obtained values of each specimen set are suited to discriminate between the two specimens of each set, in a similar manner as the stylus based surface evaluation technique. This enables the computer vision technique to be used in evaluation of surface roughness for computing surface roughness parameters in micro/nano-scale regions.

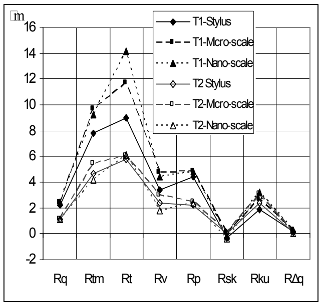

(a) Parameter values for turning

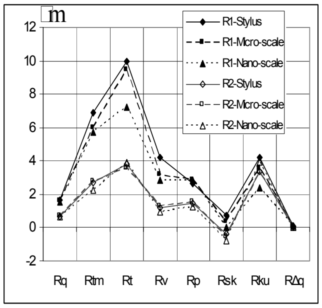

(b) Parameter values for reaming

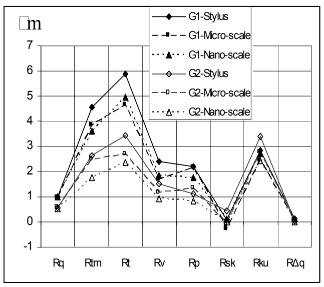

(c) Parameter values for grinding

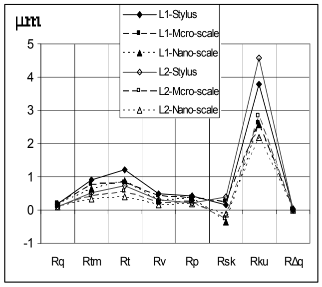

(d) Parameter values for lapping

Figure 4. Computational results of roughness parameters

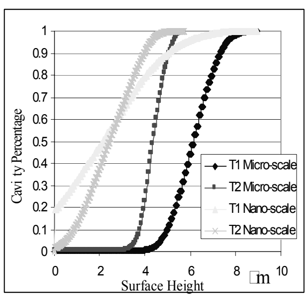

(a) Cavity graphs for turning

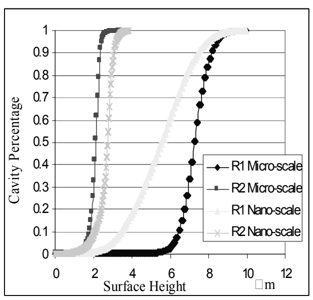

(b) Cavity graphs for reaming

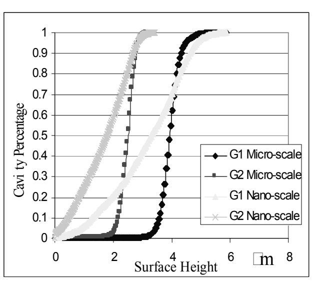

(c) Cavity graphs for grinding

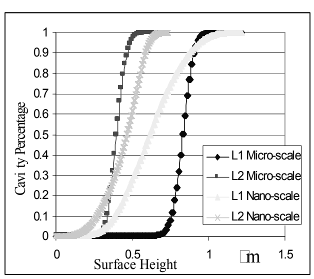

(d) Cavity graphs for lapping

Figure 5. Computational results of cavity graphs

Results on computation of cavity graphs are shown in Fig. 5. The results indicate that the specimens irregularities obtained from the nano-scale data have different forms of profile in comparison with those acquired from the micro scale data. The nano-scale based graphs gradually increase more than the micro-scale obtained graphs. This indicates that monitoring of specimens surfaces in the nano-scale region by using the proposed technique succeeds to acquire the fine surface features, such as macro-pits and macro surface irregularities.

Comparisons of the obtained cavity graphs for each specimen set show a well distinguishable profile shape of the resulting graphs, and thus it demonstrates the effectiveness of the method in the discrimination of the surface topography in both micro-scale and nano-scale regions. However, the method does not provide single numerical values to enable straight comparisons and judgments on the quality of the surface. Therefore, valid numerical descriptors obtained from this technique will enable the technique to be extensively applied in industries. In addition, the cavity graph technique does not offer assessment of the surface topography with reference to the periodicity and randomness of its irregularities. The technique of auto correlation can establish a complementary technique to overcome this limitation. Results on applying the auto correlation technique are given in Fig. 6 for the four sets of specimens.

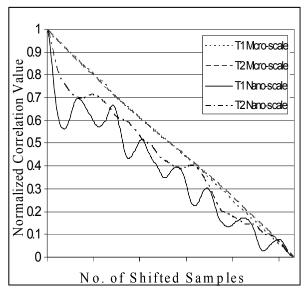

(a) Auto correlation for turning

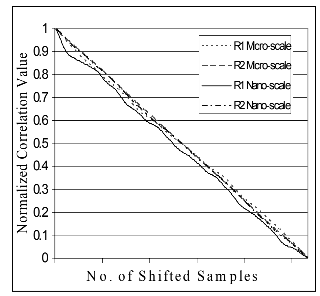

(b) Auto correlation for reaming

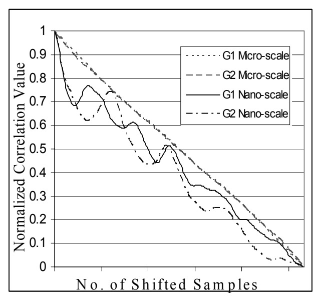

(c) Auto correlation for grinding

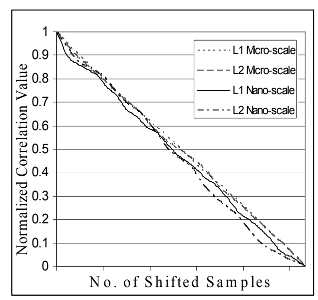

(d) Auto correlation for lapping

Figure 6. Auto correlation of monitored specimens

It is evident from the results that the micro-scale data of the specimens has generated a very similar form of graphs, which indicates that the micro-scale monitored band has failed to identify the differences in the profile irregularities of the specimens. This is because the selected specimens are generally considered as highly finished surfaces, and the arrangement of surface peaks and valleys cannot be easily identified in the micro-scale band, while the monitoring of these surfaces in the nano-scale region by using the auto correlation technique has clearly demonstrated the great capacity of the technique in identifying the periodicity and randomness of the surface texture features for each specimen in each set.

VI. CONCLUSIONS

This paper presents a vision-based approach for surface roughness assessment in micro and nano-scale regions. The proposed approach provides satisfactory results. Surface roughness parameters are obtained with adequate accuracy in comparison with the stylus based parameters. However, certain identified roughness parameters provide more accurate results than others since the definition of these parameters involves less sensitive models to local magnitude changes. The obtained values of the surface roughness parameters provide valid distinct values among the different specimens in a similar manner to the stylus based technique. No obvious change in the obtained roughness parameter values is resulted from the micro/nano regions of data in the proposed method. The adopted technique of cavity graphs succeeds to clearly provide distinguishable graph profiles with respect to the metal-cavity relationship for micro/nano-scale regions. It is found that the resulting graph shapes of the nano-scale region data incline to change more gradually. This denotes the capability of the technique for collecting the macro surface details that are invisible in micro-scale data.

The technique of auto correlation also demonstrates the great capacity in providing vital information with respect to the periodicity and randomness of the surface texture features in nano-scale data. The overall results guarantee the validity of vision data to enable surface roughness assessment. Therefore, the proposed method supports further development of the techniques for extensive applications in industries.

REFERENCES

[1] S. Lo, J. Chiu and H. Lin "Rapid measurement of surface roughness for face-milling aluminum using laser scattering and the Taguchi method" Int. J. Adv. Manuf. Technol. Vol. 26, No. 9-10, pp 1071-1077, 2005.

[2] S. Jetley and D. Selven "Applying Machining Vision to Surface Texture Analysis" IEEE Proceedings of the 36th Midwest Symposium on Circuits and Systems, Vol. 2, pp. 1456-1459, 1993.

[3] X. Li, L. Wang and N. Cai "Machine-vision-based surface finish inspection for cutting tool replacement in production" Int. J. Prod. Res., Vol.42, No. 11, 2004, pp. 2279-2287.

[4] B. Lee and Y. Tarng "Surface roughness inspection by computer vision in turning operations" Int. J. of Machine Tools & Manufacture, No. 41, pp. 1251–1263, 2001.

[5] C. Brady and Y. Wong "Surface texture indicators of tool wear– a machine vision approach" J. of Adv. Manufacturing Technology No. 17, pp.435-443, 2001.

[6] K. Lee, S. Ho, and S. Ho "Accurate estimation of surface roughness from texture features of the surface image using an adaptive neuro-fuzzy inference system", Precision Engineering, No. 29, pp.95–100, 2005.

[7] Y. Tasan, M. De Rooij and D. Schipper "Measurement of wear on asperity level using image-processing techniques" Wear, No. 25, pp.883-91, 2005.

[8] G. Al-Kindi, R. Baul and K. Gill "An application of machine vision in the automated inspection of engineering surfaces" Int. J. Prod. Res., Vol. 30, No. 2, pp. 241–253, 1992.

[9] K. Ramana and B. Ramamoothy "Statistical Methods to Compare the Texture Features of Machined Surfaces" Pattern Recognition. No. 29, pp. 1447–1459, 1996.

[10] R. Kruger-Sehm and J.A. Luna Perez "Proposal for a guideline to calibrate interference microscopes for use in roughness measurements" Int. J. of Machine Tools & Manufacture, No. 41, pp.2123–2137, 2001.

[11] Ganesha Udupa, M. Singaperumal, R. S. Sirohi and M. P. Kothiyal "Characterization of surface topography by confocal microscopy: I. Principles and the measurement system" Meas. Sci. & Technol., No. 11, pp. 305–314, 2000.

[12] Tsunemoto Kuriyagawa, Nobuhito Yoshihara, Masaru Saeki, and Katsuo Syoji "Nano-Topography Characterization of Axisymmetric Aspherical Ground Surfaces" Key Engineering Materials Vols. 238-239, pp. 125-130, 2003.

[13] D. J. Whitehouse, Surface metrology, Meas. Sci. & Technol., Vol. 8, No. 9, pp. 955–972, 1997.